

PROBLEM NO. SIE-4

Title: Damage Tolerance Analysis of Rear Wing Spar Considering the Reinforcing Effect of the Wing Skin

Objective:

To illustrate the process of estimating crack growth behavior in a structure with reinforcement in order to set inspection limits.

General Description:

This problem focuses on a damage tolerance assessment of a rear wing spar. The methodology used to analyze this problem utilized a finite element model with cracked elements to generate stress intensity factors. This approach was used to account for the reinforcing effect of the wing skin. The analysis also utilized an in-house crack growth program to generate the crack growth life.

Topics Covered: Damage tolerance assessment, cracked finite element, crack growth analysis, load spectrum development, inspection intervals

Type of Structure: wing rear spar and skin

Relevant Sections of Handbook: Section 2, 5, 11

Author: Lesley Camblin

Company Name: Structural Integrity Engineering
9525 Vassar
Chatsworth, CA 91311
818-718-2195
www.sieinc.com

Contact Point: Matthew Creager
Phone: 818-718-2195
e-Mail: mcreager@sieinc.com



Overview of Problem Description

This problem focuses on the crack growth life of a rear wing spar accounting for the reinforcing effect of the wing skins. The rear spar is C shaped. The dimensions of the vertical web, top and bottom flanges, as well as the thickness change along the span of the spar are accounted for. The bottom flange is connected to the wing skin with two staggered rows of rivets. It is assumed that a crack will initiate from one of these attachments, since the specified loading spectrum causes this flange to be under the highest tension stress.

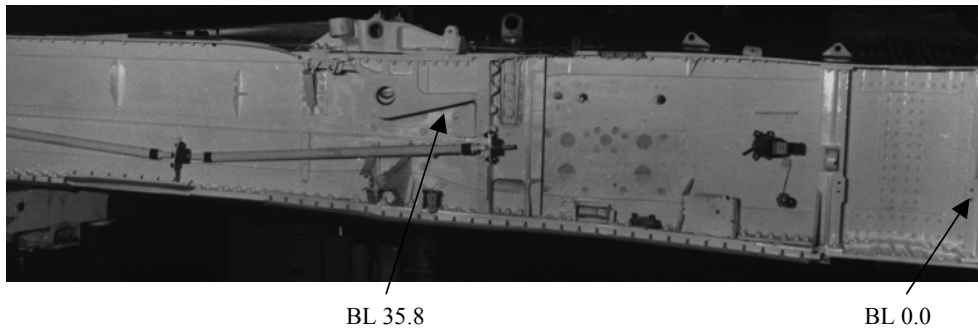


Figure SIE-4.1. Rear Wing Spar

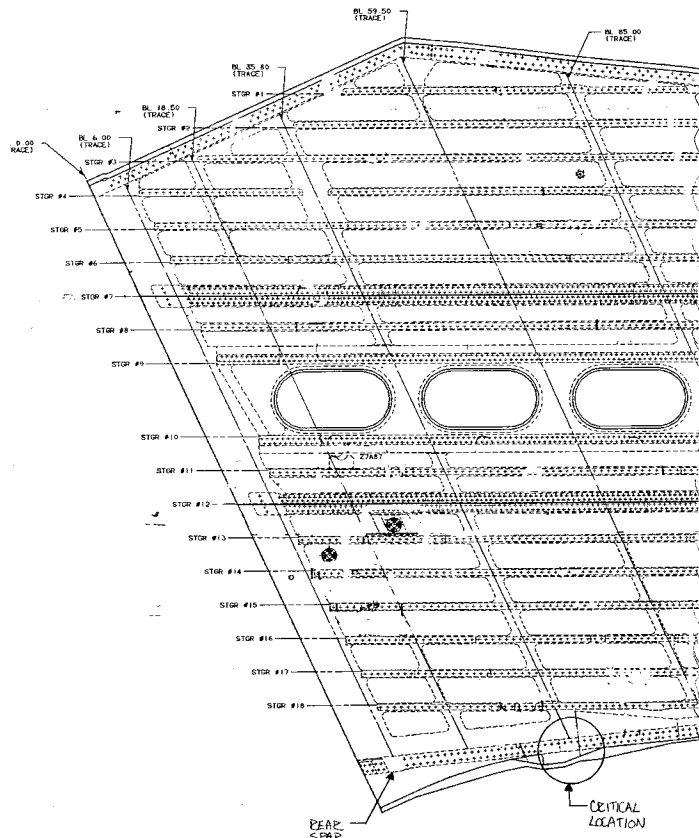


Figure SIE-4.2. Wing Lower Skin at Critical Location on Rear Wing Spar.

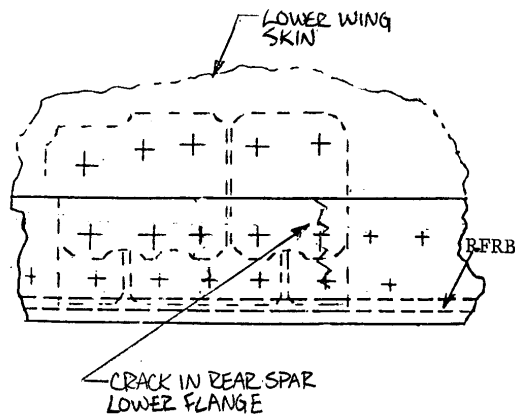


Figure SIE-4.3. View Looking Up at the Cracked Rear Spar.

Structural Model

The wing skins provide reinforcement to the assembly affecting the overall load transfer as the crack propagates. Where the overall load transfer is greatly affected by the crack, an established finite element approach is available. It is important to note that in these crack configuration cases, the crack will always be a through the thickness crack and thus a two dimensional model of the crack tip vicinity is appropriate.

The finite element approach that is used in this example employs a special cracked finite element that contains the crack tip singularity within it. A cracked finite element can be found in MSC/NASTRAN or other similar programs. The stress intensity factor is automatically generated and is uniquely defined. The overall mesh requirements are not demanding; relatively crude meshes give excellent results utilizing this element.

The proper singular behavior of stress and strain distributions from the near field solutions of linear fracture mechanics are embedded into the shape functions of the cracked element. The inter-element compatibility conditions of displacement and tractions are maintained through the use of Lagrangian multiplier techniques. Consequently, the stress intensity factors are solved directly as unknowns in the final algebraic system of equations along with the nodal displacements. It has been shown that by using only 20 to 50 degrees of freedom, the stress intensity factor can be computed using the cracked element with accuracy of one percent or better.

Although this example uses a specific cracked element, the intent of this problem is to show how to incorporate these types of elements into a damage tolerance analysis. This is why the derivations of the specific element are not presented here.

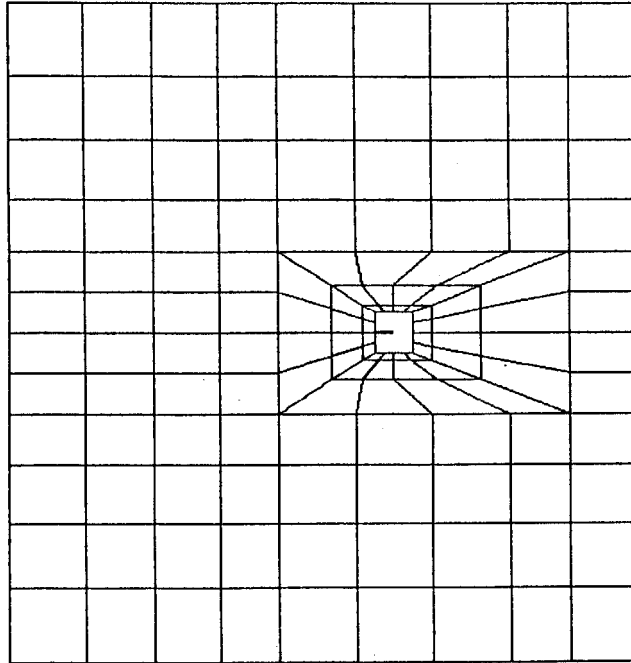


Figure SIE-4.4. Example of a Finite Element Mesh with a Cracked Element.

Model Geometry Description

For an initial crack at the rear spar to skin attachment, the fatigue crack propagation life is divided into two phases. The first phase, Phase 1, consists of a through the thickness crack starting from a rivet hole in the rear spar bottom flange in the row farthest from the web, and growing towards the edge of the flange. This is simulated as a crack emanating from an eccentric hole in a plate, as wide as the lower flange, subject to constant uniform stresses ($W = 2.443$ in., $t = 0.25$ in., $D = 0.312$ in.). In this first phase, the wing skin has negligible effects, and the crack growth analysis is performed using standard stress intensity solutions.

The second phase, Phase 2, occurs after the crack in Phase 1 reaches the edge of the flange. In this second phase, the crack becomes an edge crack growing towards the web of the spar. Phase 2 is analyzed as an edge crack in a semi-infinite plate subject to uniform stresses that change with crack length. This change in stress with crack length is due to the reinforcing effect of the wing skins.

This phase of crack growth in the rear spar was studied using the aforementioned finite element analysis with a cracked element to determine the stress intensity factor versus crack length.

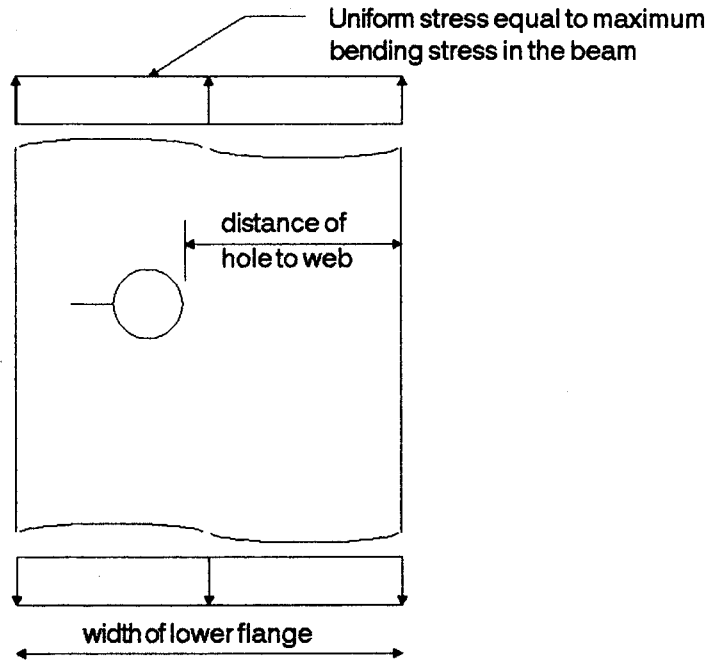


Figure SIE-4.5. Initial, Phase 1, Crack Growth Model.

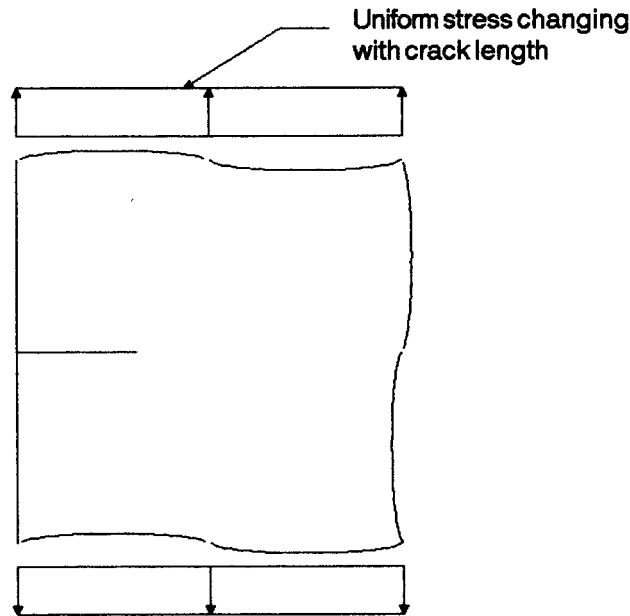


Figure SIE-4.6. Phase 2 Crack Growth Model.

In Phase 2, ten different finite element models representing the rear spar at BL35.8, each with a different crack length, were generated. The following figures show respectively the mesh for the case where the crack is partially along the flange and where the flange is fully cracked with the crack tip on the beam web.

These models utilize symmetry through the crack plane and model the structure on one side of the crack with the appropriate boundary conditions along the crack plane.

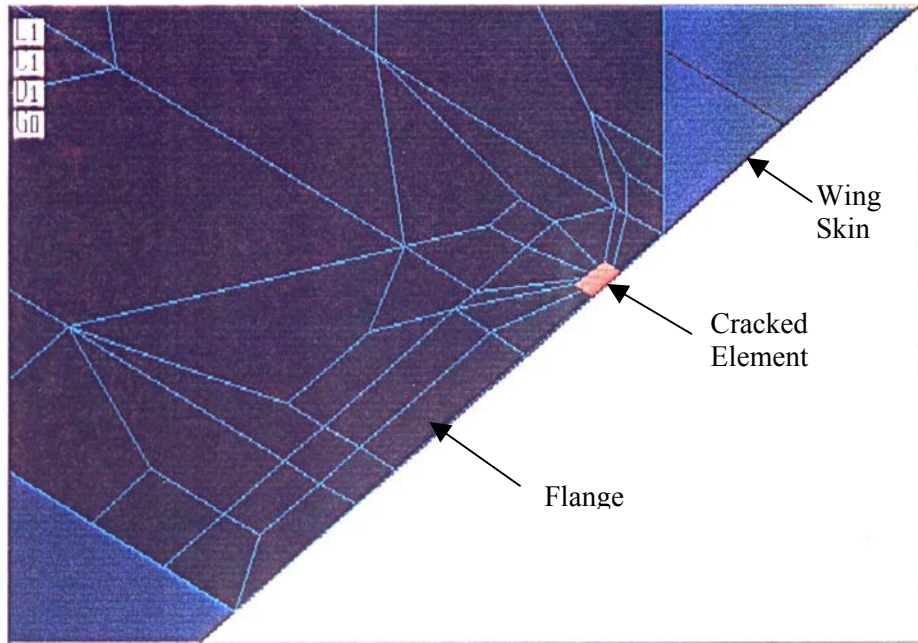


Figure SIE-4.7. Partially Cracked Flange.

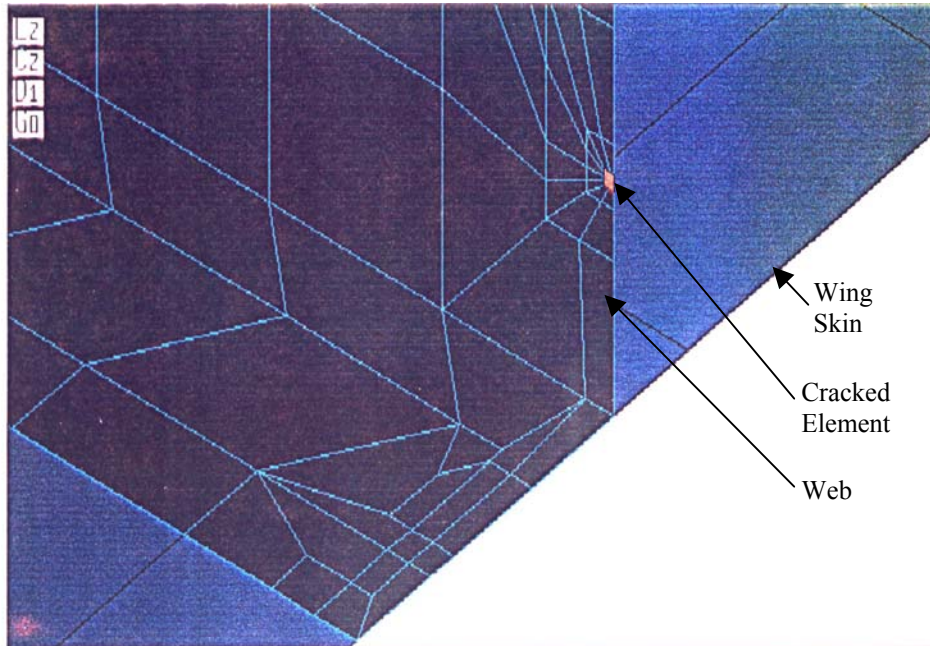


Figure SIE-4.8. Fully Cracked Flange.

The upper and lower skins were modeled as intact. It is appropriate to model these skins as intact as long as fatigue cracks will not be generated in the skins as the crack grows in the rear spar. The effect of the crack-stopper attached to the web was conservatively ignored. The applied load for the stress intensity factor analysis consisted of a unit moment applied at a distance of 24 inches from the crack. [Table SIE-4.1](#) contains the obtained stress intensity factors for various crack lengths.

Table SIE-4.1. Stress Intensity Factors for Skin Intact.

CRACK LENGTH (in.)	STRESS INTENSITY FACTOR (ksi.sqrt(in.))
1.05	4.617E-03
1.25	4.493E-03
1.45	4.053E-03
1.65	3.542E-03
1.85	3.516E-03
2.443	3.654E-03
2.943	4.578E-03
4.443	5.166E-03
6.443	4.813E-03
8.443	4.037E-03

[Figures SIE-4.9](#) and [SIE-4.10](#) show the variation of β and K/σ with length. Note the reduction in K/σ as the crack progresses through the spar flange and then increases after it gets near the spar web.

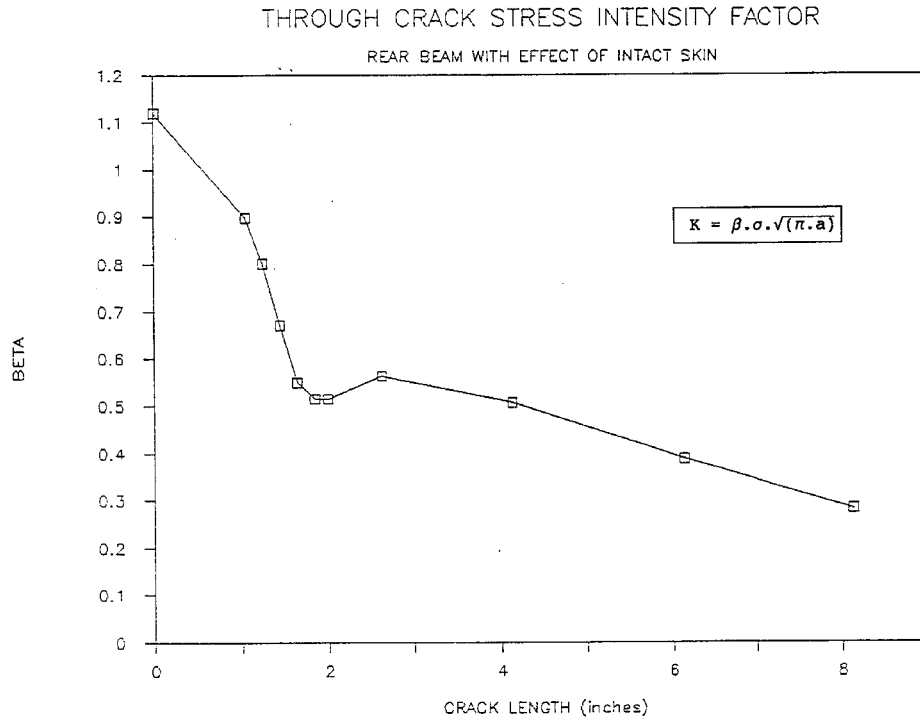


Figure SIE-4.9. Crack Length vs β .

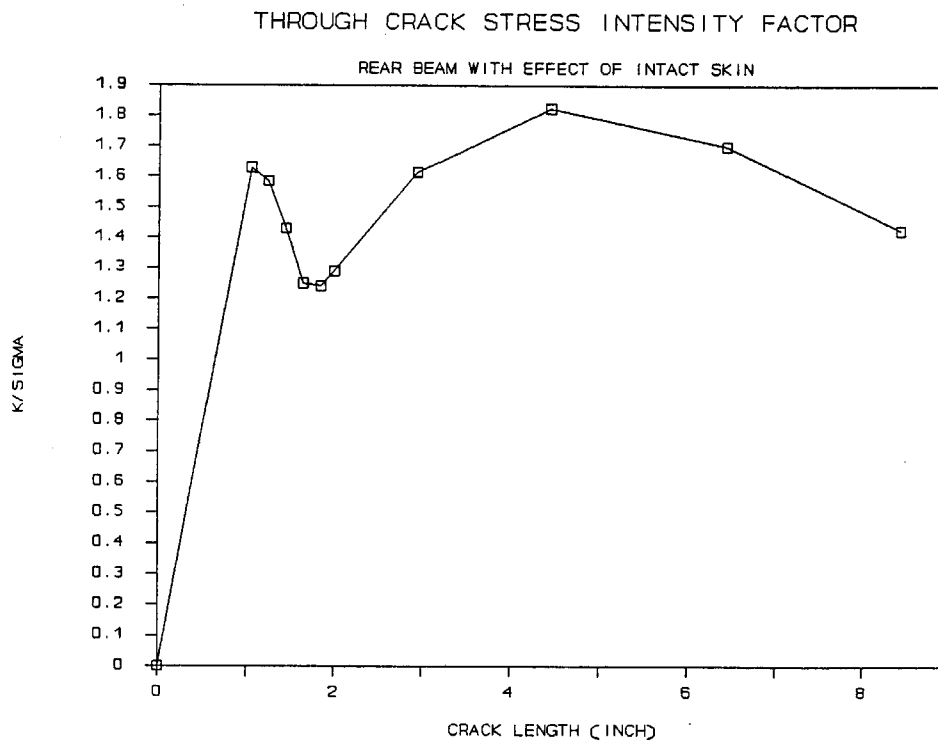


Figure SIE-4.10. Crack Length vs K/σ .

Inspection Capabilities and Crack Limits

The crack growth analysis was driven by the simple criteria that any fatigue damage is required to be discoverable prior to the failure of a critical element that could lead to the loss of the airplane. The goal of this analysis was to show that the rear wing spar and skin would have a crack growth life, with an initial through the thickness crack, greater than the design life of 20,000 hours and that the threshold inspection would be based on past experience and practice.

Structural Loading and Stress History Description

The design lifetime for the aircraft is 20,000 hours. Based on the Airplane flight profile combined with gust maneuver exceedance curves, and the stress profiles on the assembly, a stress spectrum is developed. This spectrum is defined in blocks for the analysis.

The spectrum block that was used for crack growth analysis is 500 hours long and repeated 40 times in a lifetime, so that the frequency of the highest load is 40 per lifetime. This is a conservative clipping level for the high loads, since less frequently applied loads would cause more crack growth retardation.

Based on a truncation study described below, a stress range truncation level of 1.6 ksi was used for the low loads. Due to the large number of cycles occurring in this spectrum block, first the cycles representing 100 flight hours were generated and then the 100 hour block was repeated five times with proper intermediate overloads to form the 500 spectrum block.

A truncation study was conducted for two locations located on the rear spar. [Table SIE-4.2](#) shows the growth lives as a function of the spectrum truncation level.

Table SIE-4.2. Truncation Level.

Location	Truncation Level (ksi)	Life in Hours
1	0.8	28,000
1	0.85	29,000
1	0.9	30,000
1	1.0	34,000
2	0.7	746,000
2	0.8	782,000
2	0.9	953,500

For both locations, the growth lives stabilized at an amplitude stress level truncation value of 0.8 ksi. This corresponds to a stress range truncation value of 1.6 ksi. This truncation level was used for spectrum generation of the critical location.

There are four flight types in the mission mix. The following table shows the airplane life profile. For each flight, the duration and sequence of segments are indicated. The

last column represents the percentages of design life for each segment of a flight. There are twenty different segment types.

Table SIE-4.3. Airplane Flight Profile.

SEGMENT TYPE	DESCRIPTION	TIME (MINUTE)	% TOTAL TIME
SHORT TEST FLIGHT (18% of total flights)			
20	TAKEOFF	1.0	0.14723
1	CLIMB	0.9	0.13251
2	CRUISE	13.0	1.91402
3	DESCENT	2.4	0.36338
19	A & L	5.0	0.73818
SHORT RANGE FLIGHT (21% of total flights)			
20	TAKEOFF	1.0	0.17177
5	CLIMB	1.9	0.32838
6	CLIMB	2.8	0.48098
7	CLIMB	2.4	0.41225
4	CRUISE	18.0	3.09187
18	DESCENT	1.9	0.32838
17	DESCENT	3.8	0.61897
18	DESCENT	4.8	0.79015
19	A & L	5.0	0.86885
MEDIUM RANGE FLIGHT (46% of total flights)			
20	TAKEOFF	1.0	0.38808
5	CLIMB	2.0	0.73818
6	CLIMB	2.8	1.03082
7	CLIMB	3.4	1.25147
8	CLIMB	5.0	1.84040
9	CRUISE	90.0	39.12721
15	DESCENT	3.3	1.21488
16	DESCENT	2.5	0.92020
17	DESCENT	3.5	1.28828
18	DESCENT	4.5	1.66838
19	A & L	5.0	1.84040
LONG RANGE FLIGHT (18% of total flights)			
20	TAKEOFF	1.0	0.13087
10	CLIMB	2.5	0.32718
11	CLIMB	3.7	0.48423
12	CLIMB	4.5	0.58893
13	CLIMB	8.0	1.04898
14	CRUISE	300.0	99.29188
15	DESCENT	3.4	0.44497
16	DESCENT	2.8	0.34027
17	DESCENT	3.8	0.47114
18	DESCENT	4.7	0.61510
19	A & L	5.0	0.66438

Detailed exceedance curves for the take-off segment were not generated because it was simpler to use a slightly conservative ground load for all flights. Therefore, a total of 19 gust stress exceedance curves, 19 maneuver exceedance curves, and 19 1G stresses were supplied for the critical location.

The steps in generation of the 100 hour spectrum block are described below. In steps a and b, peak and valley stresses are generated without consideration of their sequence in the spectrum block. Step h describes the inclusion of fuselage pressure.

- a. For each segment type (i.e. climb, cruise, descent, and approach and landing) the total number of excursions of positive and negative gusts and maneuvers in a spectrum block of 100 hours is determined. The total number of excursions is the product of the exceedances per flight hour at the stress truncation level and the number of blocks.
- b. There are separate exceedance curves for maneuver peaks and valleys. Gust peaks and valleys are related in that their exceedances have the same absolute values but opposite signs. For each segment type, all gust peaks and maneuver peaks and valleys are picked from respective exceedance curves on a random basis and without replacement. The total number of excursions to be picked for each exceedance curve was generated in step a. Three files of stress values are generated for each of the nineteen segments.
- c. The number of flights of each type (there are a total of four types) in the spectrum block is determined using their percentages of occurrence; their sequence is determined on a random basis.

- d. For each segment of a flight, the numbers of cycles of gusts and maneuvers are determined from the duration of the segment within a flight (as compared to the total time in that segment in the design life).
- e. For each segment of a flight, gust peaks are picked from the information generated in step b and in the order appearing there. The cycles for gust are formed by coupling each peak with its opposite value as a valley. The segment 1G stress is then added to the peaks and valleys. The stress cycles within the same segment for two flights of the same type are in general different.
- f. For each segment of a flight, maneuver peaks and valleys are picked separately from the respective information generated in step b and in the order appearing there. The segment 1G stress is then added to the peaks and valleys. The gust cycles for a segment are placed before those of maneuver.
- g. A ground stress (compression for the lower wing) is placed between each flight.
- h. For reasons of simplicity, the stresses due to fuselage pressure for various flight conditions are taken to be equal to that of the most critical pressure condition (9.0 psi). It is added to all the spectrum peaks and valleys except to the ground stresses. In general, the net effect is to increase the mean stress by this stress value.
- i. The highest peak in the block is then identified and the portion of the spectrum above it is moved to the end of the spectrum so that in the re-sequenced spectrum, the highest peak is at the beginning. In addition, the values in the spectrum not defining a peak or valley are eliminated. The re-sequencing is done to enable cycle pairing to be performed using the Rainflow method (this was accomplished with an in-house program). The cycle pairing is important to define the representative stress cycles for the crack growth analysis.

As discussed previously, a conservative clipping level is defined for the highest load. To calculate this, the combined exceedance curve of all 19 segments of gust and maneuver was generated and used to assemble a 500 hour block from the 100 hour block. The clipping level at a frequency of 40 per lifetime corresponds to the highest stress S_{500} occurring in a 500 hour spectrum; S_{500} is determined from the composite exceedance curve.

Composite exceedance curves were obtained by combining the 19 gust exceedance data, maneuver exceedance data, and 1G stress values for the 19 segment types using their associated percentage of occurrence. The composite exceedance curve was used to determine the stress level occurring 40 times in a lifetime. This was then used as the clipping level. The composite exceedance curve for the wing rear spar is shown below.

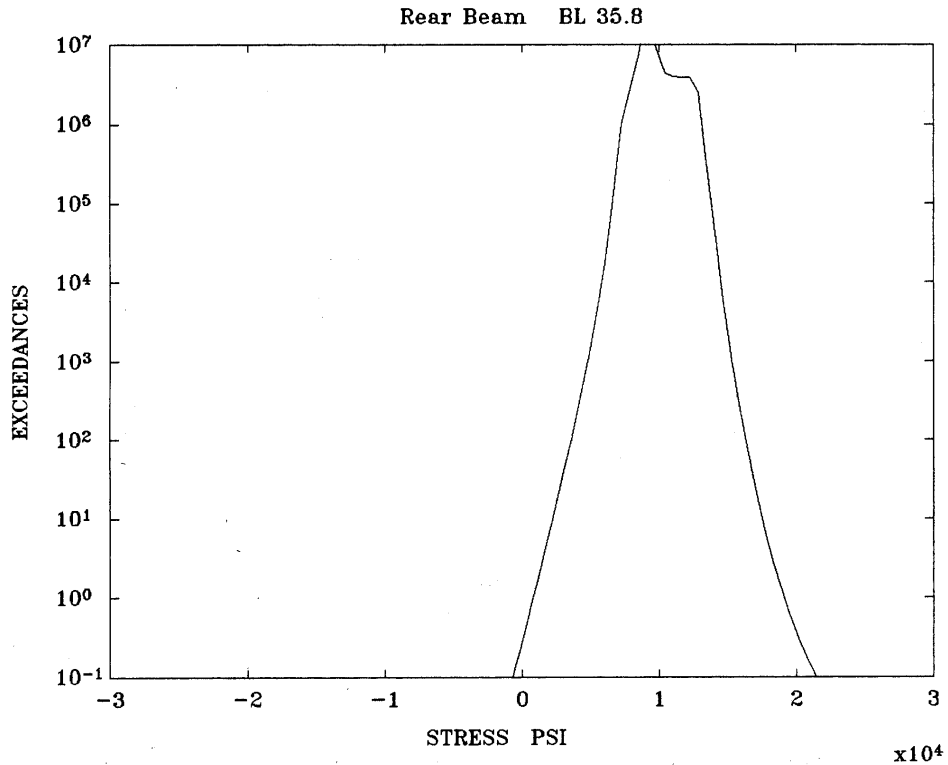


Figure SIE-4.11. Exceedance Curve for Wing Rear Spar.

S_{100} is the highest stress occurring in a 100 hour block; it can be determined either from the composite exceedance curve or from the 100 hour spectrum block. Four overloads, all larger than S_{100} , are used to extend the 100 hour block to a 500 hour block. The largest of these overloads is S_{500} . The other three overloads are determined by picking three equally distant values on logarithmic scale between S_{500} and S_{100} . The 500 hour block is formed by the following sequence:

$$S_1 + S_5 + S_3 + S_5 + S_2 + S_5 + S_4 + S_5$$

Where S_1 through S_4 are the four overloads in decreasing order and S_5 is the 100 hour spectrum block.

Material Property Description

The material properties for the rear spar, 7075-T7351LS (long/short transverse), are given below. The in-house crack growth program used the modified Willenborg retardation model and the Chang acceleration option. For the alloys used in the wing, these models have been shown to be a reasonable representation of the crack growth retardation and acceleration that occurs due to the interaction of high and low loads in the loading spectrum. The bislope representation of the crack growth rate versus ΔK was opted for the aluminum alloys. The crack growth program uses a Walker stress ratio effect model.

Table SIE-4.4. Material Properties and Growth Rate Data.

Parameter	$\Delta K < 12.1$	$\Delta K > 12.1$
C	5.044×10^{-9}	2.584×10^{-7}
n	3.189	1.608
m	0.4	0.4
q	1.0	1.0
da/dn	1.42×10^{-5}	1.42×10^{-5}
K_C	61.5	61.5
K_{IC}	29.4	29.4
F_{ty}	58	58
ΔK_{th}	0.01	0.01

Solution Technique

Although the crack growth analysis for this problem was solved using an in-house computer program, NASGRO3.0 could be also be used. Using standard stress intensity factors for Phase 1 and the stress intensity factor versus crack length chart developed with the cracked finite element for Phase 2, the crack growth analysis for this type of problem is conveniently solved using NASGRO3.0. This would require a separate crack growth run for each phase. Note that for Phase 2, the stress intensity factors versus crack length can be input into NASGRO3.0 as a table. In this example, the cycles for crack growth life will be converted into hours with the assumption of 0.67 hours per ground-air-ground (GAG) cycle.

Results

Life:

Using the relationships for b, the crack growth rate data for 7075-T7351LS, and the appropriate stress spectrum, it was found that the total crack growth duration of parts 1 and 2 up to the crack stopper on the flange is 60,000 hours corresponding to three design lifetimes. Based upon this, the initial inspection should be based upon past experience and practice and is not impacted by the damage tolerance analysis.

CRACK PROPAGATION IN REAR BEAM

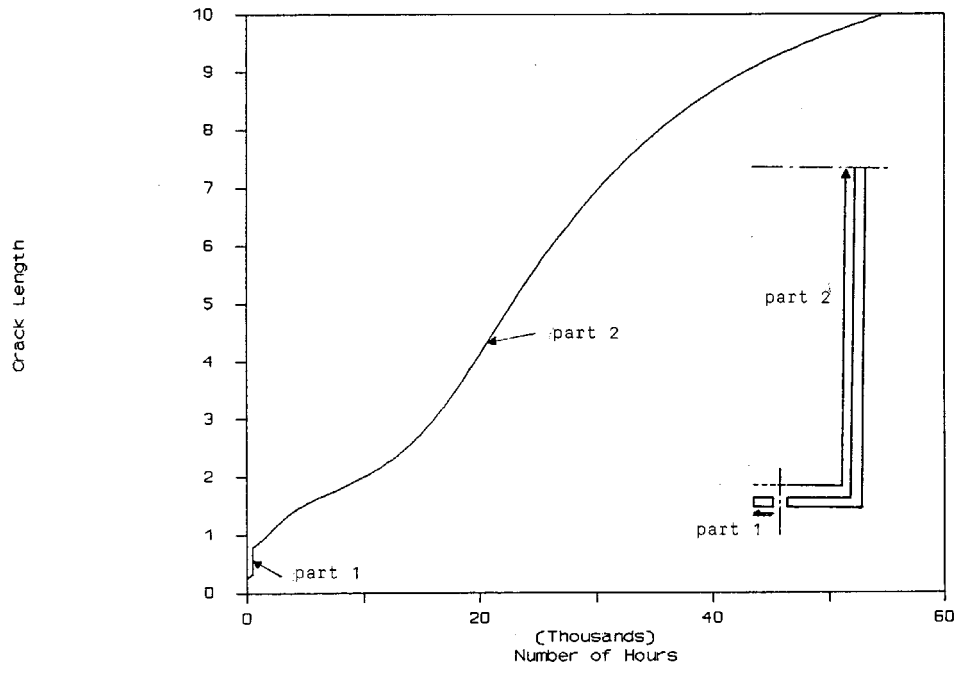


Figure SIE-4.12. Crack Growth Life for Problem SIE-4.